

May 2024

MVSBoost: An Efficient Point Cloud-based 3D Reconstruction

UMAIR HAROON ^{a,1}, AHMAD ALMUGHRABI ^a RICARDO MARQUES ^{a,b} and
PETIA RADEVA ^{a,c}

^a *Universitat de Barcelona*

^b *Computer Vision Center*

^c *Institut de Neurosciències*

ORCID ID: Umair Haroon <https://orcid.org/0000-0002-1449-1838>, Ahmad AlMughrabi
<https://orcid.org/0000-0002-9336-3200>, Ricardo Marques
<https://orcid.org/0000-0001-8261-4409>, Petia Radeva
<https://orcid.org/0000-0003-0047-5172>

Abstract. Efficient and accurate 3D reconstruction is crucial for various applications, including augmented and virtual reality, medical imaging, and cinematic special effects. While traditional Multi-View Stereo (MVS) systems have been fundamental in these applications, using neural implicit fields in implicit 3D scene modeling has introduced new possibilities for handling complex topologies and continuous surfaces. However, neural implicit fields often suffer from computational inefficiencies, overfitting, and heavy reliance on data quality, limiting their practical use. This paper presents an enhanced MVS framework that integrates multi-view 360-degree imagery with robust camera pose estimation via Structure from Motion (SfM) and advanced image processing for point cloud densification, mesh reconstruction, and texturing. Our approach significantly improves upon traditional MVS methods, offering superior accuracy and precision as validated using Chamfer distance metrics on the Realistic Synthetic 360 dataset. The developed MVS technique enhances the detail and clarity of 3D reconstructions and demonstrates superior computational efficiency and robustness in complex scene reconstruction, effectively handling occlusions and varying viewpoints. These improvements suggest that our MVS framework can compete with and potentially exceed current state-of-the-art neural implicit field methods, especially in scenarios requiring real-time processing and scalability.

Keywords. 3D Reconstruction, Multi-View Stereo, Neural Implicit Fields

1. Introduction

The pursuit of realistic and accurate 3D reconstruction has long been a focal point in the field of computer vision and graphics, finding applications across a spectrum of industries, including augmented and virtual reality (AR/VR), medical imaging, and special effects in media production. Historically, the development and implementation of Multi-View Stereo (MVS) systems [1,2] have been central to these efforts. MVS, leverag-

¹Corresponding Author: Umair Haroon, contact details.

ing photometric consistency [3], has enabled the reconstruction of complex scenes from multiple images by assessing and integrating the geometric and photometric information captured from different viewpoints.

Despite the robustness and extensive application of MVS in various scenarios, the advent of neural implicit fields [4,5] has ushered in a transformative era in 3D scene reconstruction. These methods utilize deep learning to create implicit models of scenes, essentially learning continuous volumetric fields that represent complex surfaces and structures. While they offer the advantage of handling intricate topologies and continuous surface representations without the need for explicit mesh construction, they are not without limitations. Neural implicit fields often require extensive computational resources for training and are sensitive to the diversity and quality of training data, issues that can lead to overfitting and generalized inaccuracies in practical applications.

Given the computational inefficiencies and practical limitations of neural implicit fields, there remains a significant opportunity to advance MVS techniques, especially in contexts demanding high precision, real-time processing, and efficient resource utilization. This paper introduces an enhanced MVS framework that significantly refines the traditional approach by integrating the latest advancements in camera pose estimation and sophisticated image processing techniques. By employing a structured pipeline that includes camera pose estimation via Structure from Motion (SfM), followed by point cloud densification, mesh reconstruction, and texture mapping, our method retains and enhances the practical virtues of MVS.

Our comparative studies, grounded in rigorous evaluations using the Realistic Synthetic 360 dataset [6] and Chamfer distance metrics, demonstrate the superior performance of our proposed method over existing state-of-the-art techniques, including those based on neural implicit fields. This paper details a novel MVS-based approach that effectively combines scalability, accuracy, and computational efficiency.

The remainder of this paper is organized as follows: Section 2 reviews the relevant literature, Section 3 describes our methodology, Section 4 discusses the experimental setup and presents our results, and Section 5 concludes with a summary of our findings and discusses avenues for future research.

2. Related Work

Pursuing realistic and accurate 3D reconstruction has been a focal point in computer vision and graphics, with applications in augmented and virtual reality, medical imaging, and media production. MVS systems and neural implicit fields have significantly contributed to advancing 3D reconstruction techniques. Moreover, despite these advancements, time complexity, detailed and accurate reconstruction, and the training time for neural implicit fields are still in open discussion.

MVS is a well-established technique to reconstruct dense 3D scene representations from overlapping images. Traditional MVS methods typically rely on comparing RGB image patches using metrics such as Normalized Cross-Correlation (NCC), Sum of Squared Differences (SSD), or Sum of Absolute Differences (SAD) [7]. In recent years, PatchMatch-based MVS approaches [8] have become popular due to their high parallelism and robust performance [9,10].

The emergence of deep learning has resulted in significant progress in MVS. MVS-Net [11] constructs cost volumes by warping feature maps from neighboring views and

utilizes 3D Convolutional Neural Networks (CNNs) to regularize the cost volumes. To address the memory consumption of 3D CNNs, R-MVSNet [12] sequentially regularizes 2D cost maps using a gated recurrent network. Other approaches [13,14] incorporate coarse-to-fine multi-stage strategies to refine the 3D cost volumes progressively. PatchmatchNet [15] introduces an iterative multiscale PatchMatch strategy in a differentiable MVS architecture. More recently, TransMVSNet [16] integrates Transformers to aggregate long-range context information within and across images. Still, matching pixels in low-texture or non-Lambertian areas remains challenging, and errors can accumulate from the subsequent point cloud fusion and surface reconstruction steps.

2.1. Neural Implicit Fields

In recent years, neural implicit fields have become increasingly popular for multi-view 3D surface reconstruction. The reason for this growth can be attributed to the introduction of differentiable rendering of implicit functions training methods. In early works, surface rendering procedures were relied upon, wherein the color of a pixel was estimated using the radiance of a single point in the volume [?,17]. However, these methods have been surpassed by training procedures based on volume rendering, with multiple samples being taken via ray marching.

The technique of volumetric ray marching, introduced in the pioneering research on Neural Radiance Fields (NeRFs) [18], has been adapted to surface modelling, leading to significant improvements in reconstruction quality. This method estimates the color along the ray using the volume rendering integral, approximated as a sum of weighted radiances at multiple points throughout the volume. To increase the accuracy of the approximation, researchers have employed methods based on importance [19,20], uncertainty [21], or surface intersection-based [22] sampling, which have outperformed simpler strategies such as uniform sampling.

Recent advancements in neural implicit fields have introduced hybrid surface representations that enhance ray marching [23]. These representations limit the sampling space to a volume that roughly encompasses the scene in conjunction with the method of the base neural reconstruction. Researchers have optimized the selection of samples surrounding the reconstructed surface [23], which led to a superior reconstruction. Moreover, these hybrid surface representations have been used to guide the sampling of training rays, resulting in better reconstructions within the same training time. The progress in neural implicit fields has been driven by the development of more accurate and efficient sampling strategies, along with integrating these hybrid surface representations.

The main contributions of our paper are as follows: 1. **We propose a robust MVS framework:** that integrates multi-view 360⁰ imagery with advanced processing techniques to produce detailed and accurate 3D point clouds and meshes. 2. **We achieve superior performance:** outperforming existing neural implicit field approaches and traditional MVS methods in accuracy and precision, as validating through extensive testing with Chamfer distance metrics on a comprehensive dataset. 3. **We prove high computational efficiency:** by optimizing each stage of the MVS process, our approach substantially reduces the computational resources required, facilitating faster processing and greater efficiency. 4. **We illustrate the robustness on complex scene reconstruction:** since our method exhibits exceptional capability in handling occlusions and adapting to varying viewpoints, ensuring reliable and comprehensive scene reconstructions. 5. **Our**

method achieves scalability and application versatility: designed to accommodate both bounded and unbounded scenes without specific image-capturing patterns, the proposed framework adapts seamlessly across various scales and environments, making it suitable for various applications.

3. Proposed Methodology

Our study focuses on achieving precise point cloud-based 3D reconstruction of objects from multiple views.

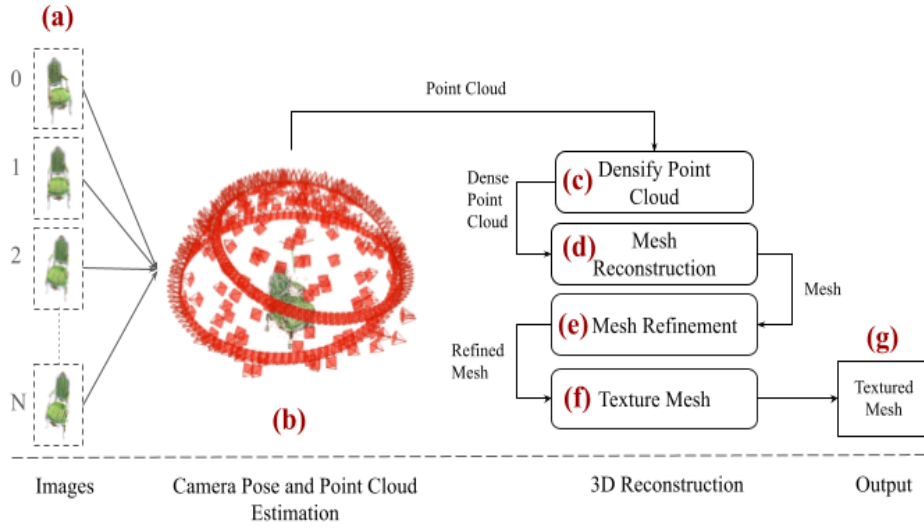


Figure 1. This figure illustrates the proposed multi-phases framework, where (a) takes multi-view 360-degree images with transparent background (i.e. object-centric RGBA images); pass them to (b) Camera Pose and Point Cloud Estimation phase, which estimates a point cloud and camera poses based on the extracted SIFT features from RGBA inputs; the point cloud passed to (c) Densify Point Cloud for obtaining a complete and accurate as possible point-cloud; (d) Mesh Reconstruction for estimating a mesh surface that explains the best the input point-cloud; (e) Mesh Refinement for recovering all fine details; (f) Texture Mesh for computing a sharp and accurate texture to color the mesh; finally (g) is the output mesh.

3.1. Overview

Our framework aims to achieve high-quality 3D reconstruction of objects in real scenarios by a given set of RGB images. Our framework relies on three distinct phases: 1. Input Images, 2. Camera and Point Cloud Estimation, and 3. 3D Reconstruction.

Fig. 1 shows a diagram representing the general overview of our proposed framework. In the first phase, (Fig. 1(a)), our framework accepts a 360⁰ scene as a set of input RGBA images. The next phase (Fig. 1(b)) extracts the SIFT features from the given images, triangulates matches of similar features where it helps to estimate the camera locations (i.e. poses), and returns a point cloud. The last phase (Fig. 1(c-f)) relies on four distinct phases. In Densify Point Cloud (Fig. 1(c)), our framework obtains a complete and accurate possible point cloud from the given point cloud by recovering the missing parts of the scene using a Patch-Match [8] approach. In the Mesh Reconstruction (Fig. 1(d)) phase, our framework uses the dense point cloud obtained from the previous steps

as its input resulting in a rough mesh. In the Mesh Refinement phase (Fig. 1(e)), the rough mesh is refined to recover fine details and larger missing parts of objects. Finally, in the Texture Mesh phase (Fig. 1(f)), the mesh is colored based on the input images.

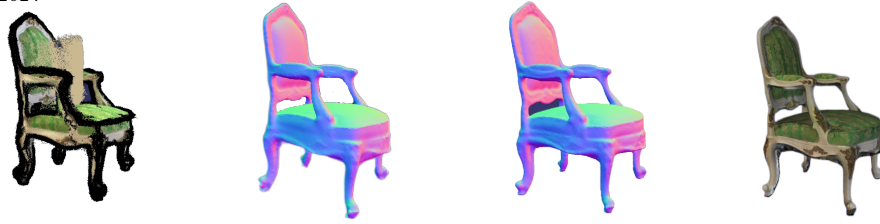
3.2. Our Proposal: MVSBoost

Our framework aims to propose rich and expressive meshes from a set of input images $\mathcal{I} = \{I_i | i = 1 \dots N_I\}$. In this section, we present the Camera Pose and Point Cloud Estimation. Secondly, we present the Densify Point Cloud, Mesh Reconstruction, Mesh Refinement, and Texture Mesh as 3D reconstruction using Point Cloud phases.

3.3. Camera Pose and Point Cloud Estimation

SfM [24] is a sequential process that reconstructs 3D structures from multiple images taken from different viewpoints. It typically involves feature extraction, feature matching, geometric verification, and an iterative reconstruction stage. The initial step involves searching for correspondences to identify scene overlap in a set of input images \mathcal{I} and determining the projections of common points in overlapping images. This process results in a collection of geometrically verified image pairs \bar{C} and a graph representing the projections of each point in the images. In the **feature extraction** step, SfM involves detecting local features $\mathcal{F}_i = \{(x_j, f_j) | j = 1 \dots N_{F_i}\}$ in each image I_i , where x_j represents the location and f_j is the appearance descriptor. These features should be invariant to radiometric and geometric changes to ensure unique recognition across multiple images. SIFT and its derivatives and learned features are considered the most robust options, while binary features offer better efficiency at the cost of reduced robustness. In the **feature matching** step, SfM identifies images capturing the same scene elements by utilizing features \mathcal{F}_i as descriptors of image appearances. Instead of exhaustively comparing all image pairs for scene overlap, SfM matches features between images I_a and I_b by assessing the similarity of feature appearances, f_j . This direct approach has a computational complexity of $O(N_I^2 \times N_{F_i}^2)$, which becomes impractical for large image datasets. Various methods have been developed to address the challenge of efficient and scalable matching. The outcome is a set of potentially overlapping image pairs $C = \{\{I_a, I_b\} | I_a, I_b \in \mathcal{I}, a < b\}$ along with their corresponding feature matches $M_{ab} \in \mathcal{F}_a \times \mathcal{F}_b$. In the **Geometric Verification** step, the third stage in SfM verifies potentially overlapping image pairs C by estimating transformations using projective geometry to ensure corresponding features map to the same scene point. Different mappings, such as homography \mathbf{H} for planar scenes, epipolar geometry with essential matrix \mathbf{E} or fundamental matrix \mathbf{F} for moving cameras, and trifocal tensor for three views, are used based on the spatial configuration. Robust techniques like RANSAC handle outlier-contaminated matches, resulting in geometrically verified image pairs \bar{C} with inlier correspondences \bar{M}_{ab} and their geometric relations G_{ab} . Decision criteria like GRIC or methods like QDEGSAC aid in determining the appropriate relation, forming a scene graph with images as nodes and verified pairs as edges, resulting in a point cloud data structure, as shown in Fig. 1(b).

May 2024



(a) Densify Point Cloud (b) Mesh Reconstruction (c) Mesh Refinement (d) Texture Mesh

Figure 2. An illustration on the 3D reconstruction module on the Chair scene.

3.4. 3D Reconstruction

In **Densify Point Cloud**, the dense point cloud extraction involves the process of enhancing a sparse point cloud created through SfM by utilizing depth map computation and Depth map fusion techniques. Depth map fusion works by generating depth maps for individual input images through feature matching across adjacent perspectives; the feature matching is conducted at various resolution levels until a detailed set of dense depth maps is obtained. Subsequently, these depth maps are consolidated into a unified dense point cloud, effectively eliminating superfluous points and noise during the fusion process, as shown in Fig. 2 (a).

Mesh reconstruction uses an MVS approach to create a mesh from a dense point cloud. The point cloud is first transformed into a tetrahedral mesh through Delaunay triangulation. Then, a graph-cut optimization determines whether each tetrahedron is inside or outside the object. Finally, the marching cubes algorithm extracts the mesh surface from the labelled tetrahedra. The resulting mesh is a seamless and accurate representation of the object’s geometry based on the original point cloud data, as shown in Fig. 2 (b).

Mesh refinement is a set of techniques used to improve reconstructed meshes’ quality. These techniques include mesh simplification, which reduces the number of vertices while preserving important details, and mesh smoothing, achieved using Laplacian or bilateral filtering to eliminate noise and outliers. Additionally, mesh denoising is used further to enhance the mesh quality through normal voting tensor filtering. Mesh optimization techniques such as vertex relaxation and edge flipping are employed to refine the quality of the triangles. These refinement processes create a clean and precise mesh that accurately represents the object’s surface characteristics, as shown in Fig. 2 (c).

Texture mesh involves mapping images onto the 3D model to create a realistic and detailed surface representation. This process significantly enhances the visual quality of the 3D model, making it suitable for various applications like virtual reality, gaming, and visualization. Texture mapping is crucial for adding color, patterns, and details to the mesh, providing a more immersive and realistic experience when interacting with the 3D model, as shown in Fig. 2 (d).

4. Experimental Results

To evaluate our proposed approach, we use the Chamfer distance [23] metric, a commonly used measure for assessing the quality of surface reconstruction. This metric calculates the average distance between each point in one point set (e.g., the reconstructed surface) and its nearest neighbor in another point set (e.g., the ground truth surface). By

combining this distance metric with the Realistic Synthetic 360 dataset, we can comprehensively assess the performance of our proposed method for 3D reconstruction tasks. These benchmark datasets provide a standardized and challenging environment to test the accuracy and robustness of our approach, ensuring that our findings are reliable and comparable to other state-of-the-art methods in the field, as shown in Table. 1.

4.1. Evaluation protocol

We followed the same evaluation protocol of Sphere NeuralWarp [23] for a fair comparison. Notably, since the Chamfer distance is sensitive to rotation, translation, and orientation between meshes, the baselines use extra information to register the predicted mesh with the ground truth mesh such as camera intrinsics information. In contrast, we use Iterative Closest Point (ICP) [25] to rigidly align the groundtruth and the reconstructed mesh avoiding the need of additional information such as camera intrinsics.

4.2. Implementation settings

We used GeForce GTX 1080 Ti/12G to run our experiments. For the Camera Pose and Point Cloud estimation phase (Fig. 1(a)), we use COLMAP [26,27]. For the feature extractor, we set a single camera option, maximum image size as 1000, default focal length as 5.2, maximum number of SIFT features as 2048, BA global function tolerance as 0.000001, and focal length ratio as $[0.1 \dots 10]$. For the 3D reconstruction phase (Fig. 1(c-f)), we use OpenMVS [28]. We set the close-holes parameter as 400, mesh smooth parameter as 5, and the maximum resolution parameter as 512.

4.3. Datasets

Our primary experiments use the widely recognized 3D reconstruction benchmark datasets, Realistic Synthetic 360 [18]. **The Realistic Synthetic 360 dataset** was created for novel view synthesis [18]. Recently, it has been repurposed to evaluate 3D reconstruction algorithms. The dataset contains eight scenes (400 images per scene; each image is 800x800px, including masks and depth images) with complex geometries and non-Lambertian materials, making it a challenging benchmark. The ground truth meshes are filtered to remove non-visible internal surfaces to ensure fair comparisons. Similarly, the reconstructed meshes also undergo a similar process.

4.4. Comparative Analysis

We compared our method to seven state-of-the-art methods on 8 scenes of the dataset. Each scene presents unique structural complexities in the reconstructed surface, which poses a challenge for standard methods to estimate the locations of high-density regions accurately. This limitation hinders the optimization process and diminishes reconstruction quality and rendering performance.

Quantitative Results: We evaluate the performance of our proposed method with seven state-of-the-art methods (COLMAP [29], NeuS [30], Sphere NeuS [23], NeuS w/ masks [30], Sphere NeuS w/ masks [23], NeuralWarp [4], and Sphere NeuralWarp [23]) on the Realistic Synthetic 360 dataset. The results are shown in Table 1. Our method shows

Methods	Chair	Drums	Ficus	Hotdog	Lego	Mats	Mic	Ship	Mean
COLMAP [29]	0.77	1.26	0.96	1.95	1.36	2.19	1.33	1.00	1.42
NeuS [30]	0.38	1.88	0.51	0.52	0.68	0.40	0.60	0.60	0.70
Sphere NeuS [23]	0.39	1.20	0.40	0.57	0.61	0.31	0.67	0.54	0.59
NeuS w/ masks [30]	0.40	0.90	0.41	0.58	0.67	0.28	0.59	0.73	0.57
Sphere NeuS w/ masks [23]	0.45	0.94	0.32	0.54	0.67	0.27	0.57	0.71	0.56
NeuralWarp [4]	0.43	3.00	0.94	1.65	0.81	1.02	0.75	1.27	1.23
Sphere NeuralWarp [23]	0.41	2.67	0.61	1.44	0.76	0.92	0.80	1.07	1.09
Ours	0.22	0.16	0.17	0.26	0.06	0.07	0.22	0.16	0.16

Table 1. A quantitative comparison of our proposed method with the state-of-the-art methods on the Realistic Synthetic 360 dataset using Chamfer distance (the lower the better).

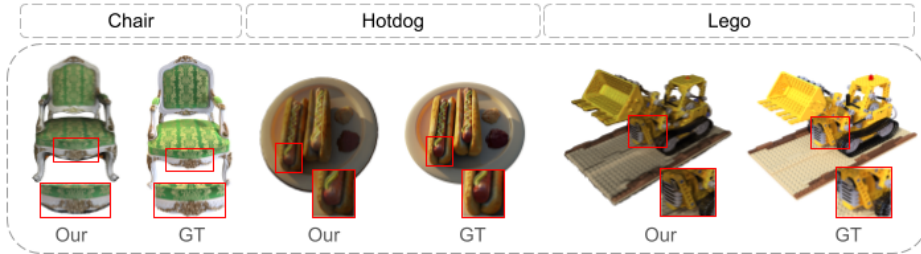


Figure 3. A side-by-side comparison showing our method’s results next to the ground truth GT from the Realistic Synthetic 360 dataset.

considerable improvements in all scenes compared to the state-of-the-art. Significant enhancements were observed consistently across all Realistic Synthetic 360 dataset scenes.

Qualitative Results: Figure 3 visually compares our method with the ground truth on the Realistic Synthetic 360 dataset. Our method generates reconstructions that are more accurate and closer to the ground truth than the state-of-the-art methods. The Realistic Synthetic 360 dataset provides high-precision ground truth 3D surface models that enable us to quantitatively evaluate the 3D reconstruction algorithms. By visually comparing the reconstructions produced by our method with the ground truth models, we can evaluate the accuracy and completeness of our results. The figure illustrates that our method can closely match the detailed geometry and surface properties of the ground truth, indicating its efficiency in reconstructing 3D objects from multi-view images.

4.5. Discussion

The experimental outcomes validate our hypothesis that traditional MVS techniques when augmented with modern computational methods and camera technologies, can surpass the performance of more recent neural approaches in real-world applications. Integrating SfM algorithms and the strategic use of 360-degree cameras have proven pivotal in enhancing the reconstruction quality. Our results also suggest that there is considerable potential to further optimize these processes, particularly in the aspects of real-time processing and handling dynamic scenes. The experimental results demonstrate that our method outperforms the state-of-the-art methods regarding Chamfer distance on the Realistic Synthetic 360 dataset. The visual results also show that our method can recon-

May 2024

struct more accurate and detailed 3D objects. These results suggest that our method is effective in 3D reconstruction tasks and can be applied to various applications such as robotics, computer vision, and virtual reality. Our results also indicate that there is significant potential to further optimize these processes, particularly in the aspects of real-time processing and handling dynamic scenes.

Complexity: One key advantage of our proposed MVS framework is its computational efficiency. By optimizing various stages of the reconstruction process, such as implementing GPU acceleration and improving the algorithms for image processing and mesh reconstruction, our method significantly reduced the computational time compared to traditional MVS methods. Furthermore, memory consumption was also minimized, enhancing the system's capacity to handle larger datasets effectively.

Corner cases: Handling of Complex Scenes and Occlusions. The enhanced MVS method performed better in reconstructing complex scenes, particularly those with significant occlusions and diverse viewpoints. The robustness of our approach was evident as it consistently maintained high levels of detail and accuracy in areas where previous methods struggled. This success is attributed to the comprehensive scene coverage provided by 360-degree imagery and the refined techniques for camera pose estimation and point cloud interpolation.

Limitations. The limitations of our method are presented, respectively: 1. Our method requires a high amount of images to have a perfect reconstruction. 2. Our method might not have a good construction for high-frequency areas such as reflections. 3. Our method may not work for different lighting conditions in the scene.

5. Conclusions and Future Work

This study successfully demonstrates the enhanced capabilities and significant advantages of our proposed MVS framework over existing neural implicit field methods. Through rigorous experimentation and analysis using the Realistic Synthetic 360 dataset and Chamfer distance metrics, our method was proven to be more accurate, precise, and efficient regarding computational resources. The novel integration of multi-view 360-degree imagery with advanced SfM techniques, alongside subsequent point cloud densification, mesh reconstruction, and texturing processes, ensures the production of high-quality 3D models. These models exhibit enhanced clarity and detail, showcasing the robustness of our approach in handling complex scenes, occlusions, and diverse viewpoints effectively. Our findings underscore the practicality of MVS in real-time and large-scale applications, suggesting that it remains a vital technology in 3D reconstruction, particularly suitable for AR/VR, medical imaging, and media production. Future work will focus on refining the MVS process, exploring more efficient algorithms for image processing, and extending the applicability to even more challenging environments. By continuing to advance the capabilities of MVS, we aim to maintain its relevance and superiority in the evolving landscape of 3D reconstruction technologies.

References

- [1] Huang PH, Matzen K, Kopf J, Ahuja N, Huang JB. Deepmvs: Learning multi-view stereopsis. In: Proceedings of CVPR; 2018. p. 2821-30.

- [2] Zhang J, Yao Y, Li S, Luo Z, Fang T. Visibility-aware multi-view stereo network. arXiv preprint arXiv:200807928. 2020.
- [3] Kim M, Seo S, Han B. Infonerf: Ray entropy minimization for few-shot neural volume rendering. In: Proceedings of CVPR; 2022. p. 12912-21.
- [4] Darmon F, Bascle B, Devaux JC, Monasse P, Aubry M. Improving neural implicit surfaces geometry with patch warping. In: Proceedings of CVPR; 2022. p. 6260-9.
- [5] Xu Q, Xu Z, Philip J, Bi S, Shu Z, Sunkavalli K, et al. Point-nerf: Point-based neural radiance fields. In: Proceedings of the IEEE/CVF conference on computer vision and pattern recognition; 2022. p. 5438-48.
- [6] Mildenhall B, Srinivasan PP, Tancik M, Barron JT, Ramamoorthi R, Ng R. Nerf: Representing scenes as neural radiance fields for view synthesis. Communications of the ACM. 2021;65(1):99-106.
- [7] Scharstein D, Szeliski R. A taxonomy and evaluation of dense two-frame stereo correspondence algorithms. International Journal of Computer Vision. 2002;47(1-3):7-42.
- [8] Barnes C, Shechtman E, Finkelstein A, Goldman DB. PatchMatch: A randomized correspondence algorithm for structural image matching. ACM Transactions on Graphics. 2009;28(3):1-9.
- [9] Galliani S, Laina I, Rother C. Mutual-suppression stereo. Computer Vision and Image Understanding. 2015;137:1-12.
- [10] Zheng Y, Chen Y, Zhang Y, Zhang J. Patch-based multi-view stereo. Computer Vision and Image Understanding. 2014;125:1-12.
- [11] Yao Y, Luo Z, Li S, Fang T, Quan L. Mvsnet: Depth inference for unstructured multi-view stereo. In: Proceedings of the European conference on computer vision (ECCV); 2018. p. 767-83.
- [12] Yao Y, Luo Z, Li S, Shen T, Fang T, Quan L. Recurrent MVSNet for High-Resolution Multi-View Stereo Depth Inference. In: Proceedings of CVPR; 2019. p. 5525-34.
- [13] Chen M, Min C, Chen Y, Wang G. Point-MVSNet: A Point-Based Multi-View Stereo Network. In: Proceedings of the IEEE International Conference on Computer Vision; 2021. p. 6187-96.
- [14] Gu Y, Chen M, Min C, Chen Y, Wang G. Cascade MVSNet: A Cascade Multi-View Stereo Network. In: Proceedings of the IEEE International Conference on Computer Vision; 2021. p. 6187-96.
- [15] Wang F, Chen M, Min C, Chen Y, Wang G. PatchmatchNet: Learned Multi-View Patchmatch Stereo. In: Proceedings of the IEEE International Conference on Computer Vision; 2021. p. 6187-96.
- [16] Ding M, Chen M, Min C, Chen Y, Wang G. TransMVSNet: Global Context-aware Multi-View Stereo Network with Transformers. In: Proceedings of CVPR; 2021. p. 6187-96.
- [17] Sitzmann V, Zollhöfer M, Wetzstein G. Scene Representation Networks: Continuous 3D-Structure-Aware Neural Scene Representations. In: NIPS. vol. 32; 2019. .
- [18] Mildenhall B, Srinivasan PP, Tancik M, Barron JT, Ramamoorthi R, Ng R. Nerf: Representing Scenes as Neural Radiance Fields for View Synthesis. In: ECCV; 2020. .
- [19] Wang P, Liu L, Liu Y, Theobalt C, Komura T, Wang W. Neus: Learning Neural Implicit Surfaces by Volume Rendering for Multi-View Reconstruction. In: NIPS. vol. 34; 2021. p. 27171-83.
- [20] AlMughrabi A, Haroon U, Marques R, Radeva P. Pre-NeRF 360: Enriching Unbounded Appearances for Neural Radiance Fields. arXiv preprint arXiv:230312234. 2023.
- [21] Yariv L, Gu J, Kasten Y, Lipman Y. Volume Rendering of Neural Implicit Surfaces. In: NIPS. vol. 34. Curran Associates, Inc.; 2021. p. 4805-15.
- [22] Oechsle M, Peng S, Geiger A. Unisurf: Unifying Neural Implicit Surfaces and Radiance Fields for Multi-View Reconstruction. In: IEEE ICCV; 2021. p. 5569-79.
- [23] Dogaru A, Ardelean AT, Ignatyev S, Zakharov E, Burnaev E. Sphere-guided training of neural implicit surfaces. In: Proceedings CVPR; 2023. p. 20844-53.
- [24] Schönberger JL, Frahm JM. Structure-from-motion revisited. In: Proceedings of the IEEE conference on computer vision and pattern recognition; 2016. p. 4104-13.
- [25] Rusinkiewicz S, Levoy M. Efficient variants of the ICP algorithm. In: Proceedings third international conference on 3-D digital imaging and modeling. IEEE; 2001. p. 145-52.
- [26] Schönberger JL, Frahm JM. Structure-from-Motion Revisited. In: Conference on Computer Vision and Pattern Recognition (CVPR); 2016. .
- [27] Schönberger JL, Zheng E, Pollefeys M, Frahm JM. Pixelwise View Selection for Unstructured Multi-View Stereo. In: ECCV; 2016. .
- [28] Cernea D. OpenMVS: multi-view stereo reconstruction library. 2020. URL: <https://cdceacave.github.io/openMVS>. 2020;5(6):7.
- [29] Schönberger JL, Zheng E, Frahm JM, Pollefeys M. Pixelwise view selection for unstructured multi-view stereo. In: ECCV. Springer; 2016. p. 501-18.

May 2024

- [30] Wang P, Liu L, Liu Y, Theobalt C, Komura T, Wang W. Neus: Learning neural implicit surfaces by volume rendering for multi-view reconstruction. arXiv preprint arXiv:2106.10689. 2021.